

Non-Muffin-Tin Energy Bands for Silicon by the Korringa-Kohn-Rostoker Method*†

ARTHUR R. WILLIAMS

IBM Watson Research Center, Yorktown Heights, New York 10598

(Received 2 October 1969)

A method is proposed for removing the "muffin-tin" restriction from the Green's function or the Korringa-Kohn-Rostoker method of band calculation and, more generally, from multiple-scattering theory as formulated by Beeby and Edwards. The method is applied to a model for crystalline silicon involving a single parameter which is adjusted to reproduce the experimental indirect gap. The numerical results are in good agreement with a large number of experiments and in particular support the view that the Δ axis is important to the reflectivity peak at 3.4 eV. (The energy separation $\Gamma_{15} - \Gamma_{25'}$ is found to be 3.04 eV.)

I. INTRODUCTION

THE Green's-function method¹ (GFM) introduced by Korringa² and by Kohn and Rostoker³ (KKR) has been used extensively for the calculation of one-electron energy bands in metals. Its use has been restricted to metals because the so-called muffin-tin approximation on which the original formulation was based is only justified when the array of ions surrounding a given ion is nearly spherical, a situation characteristic of metals, but highly uncharacteristic of semiconductors. Since the muffin-tin model assumes the one-electron potential to be constant in the region external to a set of nonoverlapping spheres centered at the ions, the fundamental measure of the model's applicability is the fraction of the total crystal volume in which we are forced to make this assumption. Even in close-packed materials, where the muffin-tin model is reasonable, it requires that the crystal potential be assumed flat in 25% of the crystal volume. Segall⁴ has shown that in the case of aluminum this approximation can lead to errors as great as 40% in particular energy differences. In a loosely packed material, such as silicon, the muffin-tin model is totally inadequate, for in this case it implies a poor assumption about 66% of the crystal volume. On the other hand the GFM possesses two important advantages; first, it is convenient to program for automatic computation⁵ and second, it is equally applicable over the entire free electron to tight-binding range. These advantages, particularly in view of the steadily growing wealth of precise experimental information on semiconductors,⁶ make it seem quite desirable to generalize the GFM to overlapping ionic potentials.

In addition to the extension of the GFM to semiconductors, the application of GFM-like techniques

(multiple-scattering theory⁷⁻⁹) to the electron-phonon problem and the study of liquids also provides motivation for a better understanding, and a relaxation, of the muffin-tin restriction. In the case of the electron-phonon interaction the saddle point in the crystal potential midway between ions constitutes a classical barrier to the electron which is raised and lowered by phonons. Any description of the interaction in terms of muffin-tin potentials implies an artificially constant barrier height—a problem easily removed by permitting the ionic potentials to overlap. In the case of liquids, although the array of nearest neighbors is quite spherical, we should like to specify the ionic separation in terms of correlation functions, in which case the non-overlap condition is a considerable inconvenience.

What follows is an attempt to clarify the physical content of the GFM and to thereby generalize the method to systems of overlapping ionic potentials. The generalization described below is actually an extension of multiple-scattering theory of which band theory is a special case; here, however, we shall concentrate on the latter for which we can compare the results of a detailed calculation with both experiment and other theories. Section II describes the physical content of the muffin-tin restriction and our proposed method for removing it. Section III describes the numerical application of this proposal to crystalline silicon.

II. THEORETICAL DEVELOPMENT

A. Derivation of Relation $(1 - KG')v|\psi\rangle = 0$

We shall be concerned here with the solution of the Schrödinger equation corresponding to a total one-electron potential V which may be decomposed into individual ionic potentials v as follows:

$$V(\mathbf{r}_1, \mathbf{r}_2) = \sum_{\mathbf{R}} v(\mathbf{r}_1 - \mathbf{R}, \mathbf{r}_2 - \mathbf{R}), \quad (1)$$

where the $\{\mathbf{R}\}$ are the ionic positions. The discussion of the GFM to follow is an extension of earlier work by Beeby⁸ and Ziman.¹⁰ Beeby obtained the GFM as a

¹ F. S. Ham and B. Segall, Phys. Rev. **124**, 1786 (1961).
² J. Korringa, *Physica* **13**, 392 (1947).
³ W. Kohn and N. Rostoker, Phys. Rev. **94**, 1111 (1954).

⁴ B. Segall, Phys. Rev. **124**, 1797 (1961).
⁵ J. S. Faulkner, H. L. Davis, and H. W. Joy, Phys. Rev. **161**, 656 (1967).

⁶ B. O. Seraphin, R. B. Hess, and N. Bottka, J. Appl. Phys. **36**, 2242 (1965).
⁷ S. F. Edwards, Proc. Roy. Soc. (London) **A267**, 518 (1962).
⁸ J. L. Beeby and S. F. Edwards, Proc. Roy. Soc. (London) **A274**, 395 (1962).
⁹ J. L. Beeby, Proc. Roy. Soc. (London) **A279**, 82 (1964).
¹⁰ J. M. Ziman, Proc. Phys. Soc. (London) **86**, 337 (1965).

special case of his more general multiple-scattering theory. Ziman elaborated on the scattering theoretic interpretation of the GFM, obtaining the formal relation $(1-KG')v|\psi\rangle=0$ which is the essence of the GFM. Since, however, both Beeby and Ziman assumed from the outset that their ionic potentials were local, spherically symmetric, and, most importantly, non-overlapping, the relevance of their results to systems of more general potentials was lost. Thus, the first task to which we address ourselves is the rederivation of Ziman's result making no assumptions beyond Eq. (1).

Our starting point is the Schrödinger equation for the one-electron wave function $\psi_{p\mathbf{k}}$ written in integral form³

$$\begin{aligned}\psi_{p\mathbf{k}}(\mathbf{r}_1) = & \int d^3r_2 d^3r_3 G_p^0(\mathbf{r}_1 - \mathbf{r}_2) \\ & \times \sum_{\mathbf{R}} v(\mathbf{r}_2 - \mathbf{R}, \mathbf{r}_3 - \mathbf{R}) \psi_{p\mathbf{k}}(\mathbf{r}_3),\end{aligned}\quad (2)$$

where p^2 is the electron's energy, \mathbf{k} its Bloch propagation vector, and G_p^0 is the standing-wave free-particle Green's function

$$G_p^0(\mathbf{r}_1 - \mathbf{r}_2) = -\frac{1}{4\pi} \frac{\cos(p|\mathbf{r}_1 - \mathbf{r}_2|)}{|\mathbf{r}_1 - \mathbf{r}_2|}. \quad (3)$$

Using the Bloch symmetry of the wave function

$$\psi_{p\mathbf{k}}(\mathbf{r} + \mathbf{R}) = \exp(i\mathbf{k} \cdot \mathbf{R}) \psi_{p\mathbf{k}}(\mathbf{r}), \quad (4)$$

we can rewrite (2) as follows:

$$\begin{aligned}\int d^3r_2 d^3r_3 \{ & \delta(\mathbf{r}_1 - \mathbf{r}_2) \delta(\mathbf{r}_2 - \mathbf{r}_3) - G_p^0(\mathbf{r}_1 - \mathbf{r}_2) v(\mathbf{r}_2, \mathbf{r}_3) \} \psi_{p\mathbf{k}}(\mathbf{r}_3) \\ = & \int d^3r_2 d^3r_3 \sum'_{\mathbf{R}} e^{(i\mathbf{k} \cdot \mathbf{R})} G_p^0(\mathbf{r}_1 - \mathbf{r}_2 - \mathbf{R}) \\ & \times v(\mathbf{r}_2, \mathbf{r}_3) \psi_{p\mathbf{k}}(\mathbf{r}_3)\end{aligned}\quad (5)$$

or more formally as

$$(1 - G_p^0 v) |\psi_{p\mathbf{k}}\rangle = G_{p\mathbf{k}}' v |\psi_{p\mathbf{k}}\rangle, \quad (6)$$

where the coordinate representation of $G_{p\mathbf{k}}'$ is given by

$$G_{p\mathbf{k}}'(\mathbf{r}_1 - \mathbf{r}_2) = \sum'_{\mathbf{R}} \exp(i\mathbf{k} \cdot \mathbf{R}) G_p^0(\mathbf{r}_1 - \mathbf{r}_2 - \mathbf{R}). \quad (7)$$

We now define the K matrix¹⁰ as the solution to the following single-center-scattering integral equation:

$$K_{\mathbf{p}} = v + K_{\mathbf{p}} G_p^0 v. \quad (8)$$

The utility of the K matrix reveals itself when we rewrite Eq. (8) as follows:

$$K_{\mathbf{p}} (1 - G_p^0 v) = v, \quad (9)$$

for we see that by operating on Eq. (6) from the left with $K_{\mathbf{p}}$ we obtain the following integral equation for

$v|\psi_{p\mathbf{k}}\rangle$:

$$(1 - K_{\mathbf{p}} G_{p\mathbf{k}}') v |\psi_{p\mathbf{k}}\rangle = 0. \quad (10)$$

This result was obtained by both Beeby and Ziman for local, spherically symmetric, nonoverlapping (i.e., muffin-tin) ionic potentials. The derivation given here reveals that these constraints on v are not necessary and that Eq. (10) is valid for any ionic potential sufficiently integrable to define a K matrix. One important feature of the result is the completeness with which the v -dependent aspects of the problem, confined to $K_{\mathbf{p}}$, are segregated from the structural aspects which are confined to $G_{p\mathbf{k}}'$.

B. Muffin-Tin Approximation

Equation (10) tells us that one-electron states in perfect crystals are completely specified by the reaction matrix $K_{\mathbf{p}}$ and the special free-particle Green's function $G_{p\mathbf{k}}'$. $K_{\mathbf{p}}$ describes the scattering of the electron by any particular ion and $G_{p\mathbf{k}}'$ describes the free-particle propagation of the electron in between scattering events. Keeping in mind the physical significance of $G_{p\mathbf{k}}'$ let us begin its mathematical description. Since it describes free-particle propagation, it will be diagonal in a momentum representation. Since, however, it describes propagation from an anisotropic array of ions, it will not be diagonal in angular momentum. These two observations and the completeness of spherical harmonics and Bessel functions allow us to write in complete generality (the spherical Bessel and Neumann functions used here are those defined by Messiah¹¹ and the spherical harmonics are the real variety defined by Ham and Segall¹¹)

$$\begin{aligned}G_{p\mathbf{k}}'(\mathbf{r}_1 - \mathbf{r}_2) = & \int_0^{+\infty} q^2 dq \sum_{L_1 L_2} \langle \mathbf{r}_1 | L_1 q \rangle \\ & \times B_{L_1 L_2}(p, \mathbf{k}, q) \langle q L_2 | \mathbf{r}_2 \rangle,\end{aligned}\quad (11)$$

where

$$\langle \mathbf{r} | L q \rangle \equiv j_l(qr) Y_L(\hat{r}) \quad (12)$$

and L is a composite index signifying both l and m , that is

$$Y_L(\hat{r}) \equiv Y_{lm}(\hat{r}) \quad (13)$$

and

$$\sum_L \equiv \sum_{l=0}^{\infty} \sum_{m=-l}^{+l}. \quad (14)$$

Equation (11) serves to define the function $B_{L_1 L_2}(p, \mathbf{k}, q)$.

In order to see the connection between the muffin-tin approximation and the GFM let us assume for a moment that the ionic potentials do not overlap.

Under this restriction on v the electron, in passing from one ionic scattering to the next, is forced to

¹¹ A. Messiah, *Quantum Mechanics* (Wiley-Interscience, Inc., New York, 1961), Vol. I.

traverse a region of zero (or, equivalently, constant) potential where its kinetic energy is exactly p^2 . From a scattering point of view then, since the electron's kinetic energy returns to p^2 before and after each ionic scattering, we may say that the scattering is elastic and, because the free-particle propagation between scatterings always takes place with kinetic energy p^2 , we may replace $G_{p\mathbf{k}}'$ by a much simpler propagator $G_{p\mathbf{k}}^E$ defined as follows:

$$G_{p\mathbf{k}}^E(\mathbf{r}_1 - \mathbf{r}_2) = \sum_{L_1 L_2} \langle \mathbf{r}_1 | L_1 p \rangle B_{L_1 L_2}^E(p, \mathbf{k}) \langle p L_2 | \mathbf{r}_2 \rangle. \quad (15)$$

The rigorous mathematical basis for this replacement is the subject of Appendix A. If we substitute $G_{p\mathbf{k}}^E$ for $G_{p\mathbf{k}}'$ in Eq. (10), we obtain

$$v|\psi_{p\mathbf{k}}\rangle = \sum_{L_1 L_2} K_p |L_1 p\rangle B_{L_1 L_2}^E(p, \mathbf{k}) \langle p L_2 | v |\psi_{p\mathbf{k}}\rangle. \quad (16)$$

If we make the additional assumption that our non-overlapping potentials are spherically symmetric, then K_p will be diagonal in angular momentum and the $\{\langle p L | v |\psi_{p\mathbf{k}}\rangle\}$ will satisfy the following relation:

$$\sum_{L_2} \{\delta_{L_1 L_2} - \langle p L_1 | K_p | L_1 p \rangle B_{L_1 L_2}^E(p, \mathbf{k})\} \times \langle p L_2 | v |\psi_{p\mathbf{k}}\rangle = 0 \quad (17)$$

which in turn implies the following determinantal relation between p and \mathbf{k} (the band structure):

$$\det\{(\langle p L_1 | K_p | L_1 p \rangle)^{-1} \delta_{L_1 L_2} - B_{L_1 L_2}^E(p, \mathbf{k})\} = 0. \quad (18)$$

The following relation between the diagonal elements of K_p and the usual scattering phase shifts and logarithmic derivatives

$$\begin{aligned} \langle p L | K_p | L p \rangle &= -p^{-1} \tan(\delta_l) \\ &= p^{-1} \frac{j_l(pr) d[R_{lp}(r)]/dr - R_{lp}(r) d[j_l(pr)]/dr}{n_l(pr) d[R_{lp}(r)]/dr - R_{lp}(r) d[n_l(pr)]/dr} \Big|_{r \rightarrow \infty} \end{aligned} \quad (19)$$

reveals that Eqs. (17) and (18) constitute the GFM in its usual form. This in turn identifies the GFM structure constants as matrix elements of the elastic Green's function $G_{p\mathbf{k}}^E$. To summarize: The physical significance of the muffin-tin approximation is the restriction to elastic ionic scattering which it implies. The mathematical significance of the muffin-tin approximation and the basis for its popularity is the elimination of the integration over interstitial kinetic energies in going from Eq. (11) to Eq. (15).

C. Overlap and Inelastic Scattering

With the physical significance of the muffin-tin approximation in hand we now turn to the more realistic but complicated situation in which the ionic potentials overlap. Because of the overlap, an electron can be

simultaneously in the field of two or more ions. From a scattering point of view this means that the electron can enter and leave the field of a given ion with its kinetic energy elevated by the potential tails of the neighboring ions. Since the overlap is anisotropic, it introduces the possibility of the electron's entering an ionic scattering with one kinetic energy and leaving with another, i.e., inelastic scattering. Accordingly, free-electron propagation in between scatterings takes place with a range of kinetic energies, thereby forcing us to use the full expression [Eq. (11)] for $G_{p\mathbf{k}}'$. Substituting Eq. (11) into Eq. (10) we obtain the generalization of Eq. (17) to non-muffin-tin potentials:

$$\begin{aligned} \langle q_1 L_1 | v | \psi_{p\mathbf{k}} \rangle &= \int_0^{+\infty} q^2 dq_2 \sum_{L_2 L_3} \langle q_1 L_1 | K_p | L_2 q_2 \rangle \\ &\quad \times B_{L_2 L_3}(p, \mathbf{k}, q_2) \langle q_2 L_3 | v | \psi_{p\mathbf{k}} \rangle. \end{aligned} \quad (20)$$

Consistent with the physical discussion above, we see that the generalized version of Eq. (10) involves off-diagonal (in q) elements of K_p corresponding to inelastic scattering and values of $B_{L_1 L_2}(p, \mathbf{k}, q)$ for $p \neq q$ corresponding to free-particle propagation at elevated kinetic energies.

Rather than attempting to solve the coupled set of integral Eqs. (20) directly we shall attempt to treat the difference between Eqs. (17) and (20) as a perturbation. To this end it is natural to introduce what we call the inelastic Green's function

$$G_{p\mathbf{k}}^I = G_{p\mathbf{k}}' - G_{p\mathbf{k}}^E. \quad (21)$$

As shown in Appendix A this decomposition is effected easily when the integral in Eq. (20) is performed using contour integration, for there is a pole at $q = p$ whose residue we identify with the elastic Green's function $G_{p\mathbf{k}}^E$; the remaining contributions to the integral provide us with an explicit expression for $G_{p\mathbf{k}}^I$. We obtain a perturbation series in $G_{p\mathbf{k}}^I$ by writing Eq. (10) in the following way:

$$v|\psi_{p\mathbf{k}}\rangle = K_p G_{p\mathbf{k}}^E v |\psi_{p\mathbf{k}}\rangle + K_p G_{p\mathbf{k}}^I v |\psi_{p\mathbf{k}}\rangle \quad (22)$$

and solving the latter by iteration to obtain

$$v|\psi_{p\mathbf{k}}\rangle = \sum_{n=0}^{+\infty} (K_p G_{p\mathbf{k}}^I)^n K_p G_{p\mathbf{k}}^E v |\psi_{p\mathbf{k}}\rangle, \quad (23)$$

or alternatively,

$$[1 - (1 - K_p G_{p\mathbf{k}}^I)^{-1} K_p G_{p\mathbf{k}}^E] v |\psi_{p\mathbf{k}}\rangle = 0. \quad (24)$$

If we define the complete scattering operator $\Gamma_{p\mathbf{k}}$ as follows:

$$\Gamma_{p\mathbf{k}} \equiv (1 - K_p G_{p\mathbf{k}}^I)^{-1} K_p, \quad (25)$$

we note that the $\{\langle p L | v | \psi_{p\mathbf{k}}\rangle\}$ satisfy a set of linear equations identical in form to Eq. (17), namely,

$$\begin{aligned} \sum_{L_2} [\delta_{L_1 L_2} - \sum_{L_3} \langle p L_1 | \Gamma_{p\mathbf{k}} | L_3 p \rangle B_{L_3 L_2}^E(p, \mathbf{k})] \\ \times \langle p L_2 | v | \psi_{p\mathbf{k}}\rangle = 0, \end{aligned} \quad (26)$$

with the corresponding determinantal relation between p and \mathbf{k} ,

$$\det\{\delta_{L_1L_2} - \sum_{L_3} \langle pL_1 | \Gamma_{p\mathbf{k}} | L_3p \rangle B_{L_3L_2}^E(p, \mathbf{k})\} = 0. \quad (27)$$

Thus the generalization of the GFM does not alter its mathematical form; it consists of replacing the K matrix of the ionic potential by the more complicated operator $\Gamma_{p\mathbf{k}}$. We can obtain an alternative and more physical interpretation of $\Gamma_{p\mathbf{k}}$ by considering the application of the GFM to a system of ionic potentials defined to be the total crystal potential in a single atomic cell. Since this decomposition of the crystal potential involves no overlap, we know that the elastic scattering approximation [Eqs. (17) and (18)] is exact in this case. By comparing Eqs. (26) and (27) with (17) and (18) we see that $\Gamma_{p\mathbf{k}}$ is simply the K matrix corresponding to the total crystal potential in a given unit cell.

D. One-Electron Energies to First Order in G^I

In this subsection we shall discuss the approximate version of Eq. (27) which has been used numerically to calculate the energy bands of silicon. We shall henceforth assume for simplicity that the individual ionic potentials are spherically symmetric. In so doing we are assuming that the anisotropy of the interstitial potential can be described by the overlap of the spherically symmetric potentials. The apparent success of the silicon energy-band calculation described in the next section suggests that this approximation is not a serious restriction.

To first order in G^I the $\{\langle pL | v | \psi_{p\mathbf{k}} \rangle\}$ satisfy the following set of linear equations:

$$\begin{aligned} \sum_{L_2} [\delta_{L_1L_2} - \sum_{L_3} (\langle pL_1 | K_p | L_1p \rangle \delta_{L_1L_3} \\ + \langle pL_1 | K_p G_{p\mathbf{k}}^I K_p | L_3p \rangle) \\ \times B_{L_3L_2}^E(p, \mathbf{k})] \langle pL_2 | v | \psi_{p\mathbf{k}} \rangle = 0. \end{aligned} \quad (28)$$

Since to zero order in G^I the following is true

$$\begin{aligned} \sum_{L_2} B_{L_3L_2}^E(p, \mathbf{k}) \langle pL_2 | v | \psi_{p\mathbf{k}} \rangle = (\langle pL_3 | K_p | L_3p \rangle)^{-1} \\ \times \langle pL_3 | v | \psi_{p\mathbf{k}} \rangle, \end{aligned} \quad (29)$$

we may rewrite Eq. (28) as follows:

$$\begin{aligned} \sum_{L_2} [\delta_{L_1L_2} - \langle pL_1 | K_p | L_1p \rangle B_{L_1L_2}^E(p, \mathbf{k}) \\ - \langle pL_1 | K_p G_{p\mathbf{k}}^I K_p | L_2p \rangle (\langle pL_2 | K_p | L_2p \rangle)^{-1}] \\ \times \langle pL_2 | v | \psi_{p\mathbf{k}} \rangle = 0. \end{aligned} \quad (30)$$

The corresponding determinantal relation between p and \mathbf{k} is the following:

$$\begin{aligned} \det[\langle pL_1 | K_p | L_1p \rangle)^{-1} \delta_{L_1L_2} - B_{L_1L_2}^E(p, \mathbf{k}) \\ - (\langle pL_1 | K_p | L_1p \rangle)^{-1} \langle pL_1 | K_p G_{p\mathbf{k}}^I K_p | L_2p \rangle \\ \times (\langle pL_2 | K_p | L_2p \rangle)^{-1}] = 0. \end{aligned} \quad (31)$$

Although the first two terms in Eq. (31) appear to be just the GFM [Eq. (18)], there is an important difference which we wish to emphasize. The phase shifts entering Eq. (18) are those of a muffin-tin potential whereas those entering Eq. (31) are those of a potential which in principle can be of arbitrary range. In other words, as formulated here, the first correction to the GFM due to overlap is simply the contribution of the "tail" of the ionic potential to the phase shifts. Our application of Eq. (31) to silicon has shown that this contribution is quite significant and that the third term in Eq. (31) can be neglected if there is only a moderate amount of overlap.

The neglect of the inelastic corrections constitutes a very attractive approximation in that the degree of interstitial potential variation found in close-packed structures can be accounted for with virtually no change in existing GFM computer programs. Therefore, we shall try to explain why and under what conditions the first- and higher-order terms in G^I may be neglected. Consider the evaluation of $\langle pL_1 | K_p G_{p\mathbf{k}}^I K_p | L_2p \rangle$ in a coordinate representation. We define the coordinate representation of $G_{p\mathbf{k}}^I$ as follows:

$$G_{p\mathbf{k}}^I(\mathbf{r}_1 - \mathbf{r}_2) \equiv \sum_{L_1L_2} Y_{L_1}(\hat{r}_1) B_{L_1L_2}^I(p, \mathbf{k}, \mathbf{r}_1, \mathbf{r}_2) Y_{L_2}(\hat{r}_2). \quad (32)$$

As is shown in Appendix B, $\langle pL | K_p$ is related to the appropriately normalized solution of the single center Schrödinger equation, $R_{lp}(\mathbf{r})$, in the following way:

$$\langle \mathbf{r} | K_p | Lp \rangle = Y_L(\hat{r}) \langle \mathbf{r} | v | R_{lp} \rangle. \quad (33)$$

Thus, as expected, the first-order inelastic correction is an overlap integral:

$$\begin{aligned} \langle pL_1 | K_p G_{p\mathbf{k}}^I K_p | L_2p \rangle = \int_0^{+\infty} r_1^2 dr_1 r_2^2 dr_2 \langle R_{l_1p} | v | r_1 \rangle \\ \times B_{L_1L_2}^I(p, \mathbf{k}, \mathbf{r}_1, \mathbf{r}_2) \langle r_2 | v | R_{l_2p} \rangle. \end{aligned} \quad (34)$$

The inelastic corrections are small, because, as shown in detail in Appendix A, $B_{L_1L_2}^I$ is given approximately by the following:

$$B_{L_1L_2}^I(p, \mathbf{k}, \mathbf{r}_1, \mathbf{r}_2) \approx (r_1 + r_2 - R_{NN})^2 \Theta(r_1 + r_2 - R_{NN}), \quad (35)$$

where R_{NN} is the nearest-neighbor distance and Θ is the Heavyside step function. The importance of Eq. (35) is revealed by examining contributions to the integral in Eq. (34) from various portions of the r_1, r_2 plane which appears in Fig. 1. We first note that B^I is nonzero only in region III. This is consistent with the KKR result, which in the present terminology is that $G_{p\mathbf{k}}^I$ is equal to $G_{p\mathbf{k}}^E$ in region I. The usual formulation of the GFM eliminates the contribution of inelastic scattering by insisting that the product $v(r_1)v(r_2)$ vanish outside of region I; this is the muffin-tin restriction. The importance of our result, Eq. (35), is that, although $G_{p\mathbf{k}}^I$ does not exactly equal $G_{p\mathbf{k}}^E$ in the overlap

region, the difference between the two, namely, G_{pk}^I , is small precisely where we expect the product $v(r_1)v(r_2)$ to be largest (near $r_1=r_2=R_{NN}/2$). This is merely the mathematical way of saying that to lowest order in the tail of the ionic potential we may add up the effects of scattering off several of them linearly.

E. Alternative Interpretations of First-Order Formalism

Equation (31) can be obtained via several routes each of which offers additional insight into the final result. In an effort to gain this insight without introducing additional mathematics we shall describe verbally two such alternative derivations. The simplest derivation by far is to simply minimize the KKR functional $v - vGv$ using solutions of the single center Schrödinger equation as trial functions (admitting from the outset that individually they are not solutions of the wave equation). Thus, the first-order formalism [Eq. (31)] retains the desirable variational character of the usual GFM.

A third and more physical route to Eq. (31) consists of making the following degenerate-kernel approximation in Eq. (20):

$$\langle q_1 L | K_p | L q_2 \rangle \approx \langle q_1 L | K_p | L p \rangle (\langle p L | K_p | L p \rangle)^{-1} \times \langle p L | K_p | L q_2 \rangle. \quad (36)$$

The first-order formalism may therefore be viewed as the approximation of the matrix element for the complicated scattering process involving three energies by the product of two simpler matrix elements, each involving only two energies. We note that this approximation is correct to first order in the degree of inelasticity $q - p$ and is therefore appropriate to the physical problem at hand. This interpretation of the first-order formalism also relates it to another description of the same problem by this author.¹²

We conclude this section with a comparison of the approach taken here with that taken by Bross and Anthony¹³ and by Beleznay and Lawrence.¹⁴ The latter authors decompose the crystal into a sum of deep spherically symmetric potentials centered on the ions and a, relatively speaking at least, weak interstitial potential. The Green's function describing propagation between the deep potentials is then corrected for scattering by the interstitial potential. This approach suffers the disadvantage that for deep potentials of sufficiently short range to insure near spherical symmetry the complementary interstitial potential is quite large. Obtaining the Green's function for propagation through such a potential is a complete band-structure calculation in itself (similar to a pseudopotential calculation for both energies and wave functions). As

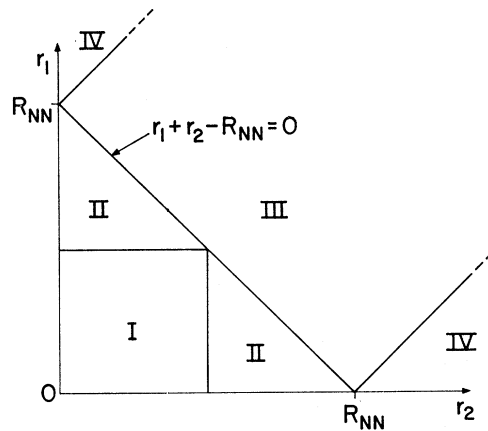


FIG. 1. The r_1, r_2 plane discussed in conjunction with Eq. (34).

mentioned below, however, the scheme presented here requires a considerable amount of computation so that probably neither approach is qualitatively superior.

II. APPLICATION TO SILICON

A. Physical Model

The physical model used here is the screened-ion model due to Heine and Abarenkov (HA).¹⁵ According to this model the ionic core (the nucleus and the ten inner electrons in the case of silicon) is a black box whose scattering properties we are willing to take as given to us by atomic or ionic (not crystalline) experimental data. The remainder of the model consists of an effective one-electron potential arising from the ionic Coulomb potential as screened by the sea of noncore electrons. To describe the screening we believe that linear dielectric screening (especially when empirically adjusted) is both better and a great deal simpler than a self-consistent Hartree-Fock-Slater treatment. Conceptually therefore our model is identical to that used by Kane¹⁶; our implementation of this basic idea is, however, somewhat different.

As far as the ionic core is concerned, we assume that it gives rise to the following l -dependent one-electron potential:

$$v_l(r) = -r^{-1}[10e^{-r/r_{lc}} + 4]. \quad (37)$$

The $\{r_{lc}\}$ may be interpreted as core radii and are adjusted so that $v_l(r)$ produces the experimental term values¹⁷ of S_i^{+3} . We have replaced the square well of the Heine-Abarenkov method by a Yukawa potential, because, for a small additional amount of computation, our parametrization (the $\{r_{lc}\}$) is much less l - and energy-dependent (a numerical comparison appears in Table I).

¹² A. R. Williams, Phys. Letters 25A, 75 (1967).

¹³ H. Bross and K. H. Anthony, Phys. Status Solidi 22, 667 (1967).

¹⁴ F. Beleznay and M. J. Lawrence, J. Phys. G 1, 1288 (1968).

¹⁵ V. Heine and I. Abarenkov, Phil. Mag. 9, 451 (1964).

¹⁶ E. O. Kane, Phys. Rev. 146, 558 (1966).

¹⁷ J. McDougall, Proc. Roy. Soc. (London) A138, 550 (1932).

TABLE I. Effective square-well depths (Ref. 16) and core radii which reproduce the atomic levels of S_i^{+++} (Ref. 17).

l	Atomic level (Ry)	Effective square-well depth (Ry)	Core radius (Å)
0	-3.32	-1.74	0.281
0	-1.55	-1.46	0.279
0	-0.899		0.278
0	-0.59	-1.22	
1	-2.66	-3.37	0.275
1	-1.33	-3.59	0.276
1	-0.798		0.274
1	-0.53	-3.67	
2	-1.86	-10.3	0.285
2	-1.04	-10.4	0.281
2	-0.662		0.281
2	-0.46	10.5	
0	-2.3	-1.59	0.280
1	-2.3	-3.43	0.275
2	-2.3	-10.3	0.285

Our treatment of the many-electron screening effects is also similar to that of Kane and HA in that it is based on the linear screening of the Coulomb tail by the exchange-corrected random-phase-approximation (RPA) dielectric constant. Here, again, however, our implementation of the basic idea is somewhat different. The many-electron effects cause the "4" in Eq. (37) to become a function of r , call it $z_t(r)$, which is 4 at the origin and falls to zero at some distance of the order of R_{NN} , the nearest-neighbor distance. If we make the rather weak assumption that it falls to zero at R_{NN} , the question becomes how does $z_t(r)$ get from 4 at $r=0$ to 0 at $r=R_{NN}$. The results of three theories for this curve are shown in Fig. 2. It will be noted that for all three the curve is linear for small r . Since a linear contribution to $z_t(r)$ is a constant contribution to the potential, the slope of this linear portion of the curve is the so-called core shift. As Phillips¹⁸ has pointed out, the band structure is extremely sensitive to this quantity and as Ziman¹⁹ has shown, various theories lead

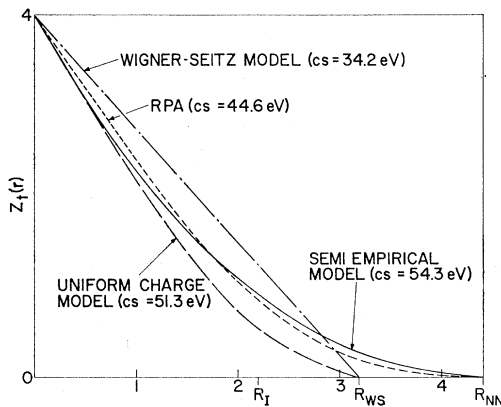


FIG. 2. $z_t(r)$ for silicon as given by three theories and the semi-empirical $z_t(r)$ used in computing the band structure; cs indicates the core shift implied by $dz_t/dr_{(r=0)}$ in each case.

¹⁸ J. C. Phillips, Phys. Rev. 125, 1931 (1962).

¹⁹ J. M. Ziman, Proc. Phys. Soc. (London) 91, 701 (1967).

to widely differing values for it. The reason that this quantity is so difficult to calculate is that it is fundamentally a matter of many-electron correlation; in silicon, for example, it may be thought of as the inverse of the distance between any one electron when it is in the core and the remaining three which, together with the one, keep the given cell neutral. Because of this combination of sensitivity and theoretical uncertainty, we have chosen to treat the core shift as an adjustable parameter by taking $z_t(r)$ to be of the following form:

$$z_t(r) = 4[(1-\alpha)(1-r/R_{NN})^2 + \alpha(1-r/R_{NN})^3], \quad r < R_{NN}$$

$$= 0, \quad r > R_{NN}. \quad (38)$$

The motivation for the functional form is that it depends on a single parameter which is related most directly to the core shift and is simultaneously a reasonable approximation to $z_t(r)$ as given by the RPA outside the core. Despite the obvious advantages of introducing greater flexibility into the model by means of additional parameters, it was felt that, since a large part of the motivation for this calculation is to establish the worth of an otherwise untested method of calculation, we should minimize the probability that any agreement with experiment obtained might be ascribed to the flexibility of the model. The numerical implications of this model with $\alpha=0.219$ are described in the next subsection.

B. Numerical Results

The results of the first-order formalism applied to the model potential described in the previous section are listed in Table II²⁰⁻²⁶ along with the corresponding quantities as inferred from experiment and as calculated by Herman²⁰ and by Kane.¹⁶ There are two important implications of the degree of agreement obtained. First the contention of several authors^{16,27-31} that the $\Gamma_{25}' - \Gamma_{15}$ energy difference is ≥ 3 eV and that as a result the Δ axis is a strong contributor to the reflectivity peak at 3.4 eV is supported by this calculation. Dresselhaus's²² analysis of this peak suggests that the experimental value for this separation is 3.0 ± 0.1 eV

²⁰ F. Herman, R. L. Kortum, C. D. Kuglin, and R. A. Short, *Quantum Theory of Atoms, Molecules, and the Solid State* (Academic Press Inc., New York, 1966).

²¹ A. Frova and P. Handler, Phys. Rev. Letters 14, 178 (1965).

²² G. Dresselhaus and M. S. Dresselhaus, Phys. Rev. 160, 649 (1967).

²³ J. C. Hensel and G. Feher, Phys. Rev. 129, 1041 (1963).

²⁴ J. C. Hensel, H. Hesagawa, and M. Nakayama, Phys. Rev. 138, A225 (1965).

²⁵ D. H. Tomboulian and D. E. Bedo, Phys. Rev. 104, 590 (1956).

²⁶ G. Feher, Phys. Rev. 114, 1219 (1959); J. Phys. Chem. Solids 8, 486 (1959).

²⁷ J. C. Phillips, Solid State Phys. 18, 55 (1966).

²⁸ D. Brust, Phys. Rev. 139, A489 (1965).

²⁹ M. L. Cohen and T. K. Bergstresser, Phys. Rev. 141, 789 (1966).

³⁰ M. Cardona and F. H. Pollak, Phys. Rev. 142, 530 (1966).

³¹ V. Gerhardt, Phys. Rev. Letters 15, 401 (1965).

with which our value of 3.04 eV is in good agreement. The low value of 2.75 ± 0.05 eV obtained by Herman²⁰ may relate to an unjustified faith in the ability of Hartree-Fock theory to predict quantities like the core shift. The value 2.83 eV for the energy separation $L_1 - L_3$ appears to be $\sim 10\%$ too small, but the sensitivity of these levels to details of the potential as discussed by Herman²⁰ and confirmed by the author suggests that a minor increase in the flexibility of the model might eliminate this problem. The reason for not attempting this here was given above.

The second implication of our results which we would like to emphasize is the general support given both the semiempirical model and the method of calculation by the fact that the adjustment of a single parameter yields values for 12 experimentally measured quantities with an average discrepancy of less than 10%. When it is recalled that Kane¹⁶ used six parameters in an attempt to fit the gap and the five mass constants exactly and still obtained a value for B 40% greater than the experimental value, the agreement obtained here seems surprisingly good.

The author would like to mention at this point that the completely empirical approach taken by Dresselhaus²² greatly facilitates efforts to relate band parameters to optical data. A good example of this is the $X_1 - X_4$ energy separation which has been identified with the optical structure at 4.2 eV. This identification has led to estimates of the energy difference of ≥ 4.0 eV whereas Dresselhaus shows that the optical structure is consistent with an energy separation of 3.75 ± 0.2 eV.

Finally, we should like to mention three points of practical interest. First, it was found that the sum over

TABLE II. Numerical results for the band parameters of silicon (energies in eV).

Band param.	Herman	Kane	Williams	Expt.
$\Delta_1^m - \Gamma_{25}'^a$	1.13	1.15	1.13	1.13 ^b
$X_1 - \Gamma_{25}'$	1.30		1.28	
$L_1 - \Gamma_{25}'$	2.05 ± 0.2		1.75	
$\Gamma_{15} - \Gamma_{25}'$	2.7 ± 0.05	3.2	3.04	3.0 ± 0.01^c
$L_1 - L_3'$	3.2 ± 0.2	2.9	2.83	3.2 ± 0.01^c
$\Gamma_2' - \Gamma_{25}'$	3.8 ± 0.4	3.3	3.28	3.75 ± 0.2^c
$X_1 - X_4$	4.05 ± 0.05	4.1	3.86	3.75 ± 0.2^c
$L_3 - L_5'$	5.0 ± 0.05	5.3	4.90	5.3 ± 0.4^c
A^e		-4.55	-3.72	-4.28 ± 0.02^d
B		-1.07	-0.94	-0.75 ± 0.04^d
N		-9.16	-7.52	-9.36 ± 0.1^d
$m_{11}^{-1}f$		+1.09	+1.06	$+1.09 \pm 0.02^e$
m_1^{-1}		+5.06	+4.63	$+5.25^e$
Bandwidth			11.84	16.7 ± 0.1^i
$k(\Delta_1^m)^h$	0.81		0.834	0.85 ± 0.03^j

^a Δ_1^m is the lowest energy in the conduction band.

^b References 20 and 21.

^c Reference 22.

^d Reference 23.

^e A , B , and N are the valence band mass constants as defined by Hensel and Feher (Ref. 19).

^f m_{11}^{-1} and m_1^{-1} are the ratios of the inverse effective masses of the conduction band minimum to the free electron value.

^g Reference 24.

^h $k(\Delta_1^m)$ is the fraction of the distance to X along Δ at which the conduction-band minimum is located.

ⁱ Reference 25.

^j Reference 26.

TABLE III. Convergence of energies (eV) with increasing l_{\max} .

l_{\max}	$E(\Gamma_{25}')$	$E(\Delta_1^m)$	GAP	$E(AL)^a$
0				-1.428
1	2.247	5.234	2.987	-2.343
2	-0.253	0.820	1.073	-2.447
3	-0.315	0.750	1.065	-2.449
4	-0.386	0.742	1.128	-2.449

^a Energies calculated by Segall (Ref. 4) corresponding to a muffin-tin model for aluminum.

lattice sites occurring in the inelastic term [Eq. (A17)] could be truncated to include only nearest neighbors without noticeable effects. Second, although the inelastic correction by itself does not raise computation time seriously, the application of the GFM to extended ionic potentials such as required for silicon does require much more computer time than does a similar application to say aluminum. This increase is due to the fact that ionic potentials of greater range couple more angular momenta (see Table III). Since the dimension of the secular equation goes as $(l_{\max} + 1)^2$, and the time required to evaluate determinants increases as the dimension cubed, this is a nontrivial matter. The program presently in use requires of the order of a minute per \mathbf{k} on an IBM-360/67; the same program adapted to aluminum takes 0.03 minutes per \mathbf{k} .

Third and last, the sensitivity of the energy bands to details of the ionic potential, as described by Table IV, demonstrates the advantage of both the semiempirical approach generally and, more specifically, the use of Yukawa potentials in place of square wells in treating the ionic core.

ACKNOWLEDGMENTS

The author particularly wishes to thank his thesis advisor, Dean Harvey Brooks, for much encouragement and advice. He also wishes to thank Professor Henry Ehrenreich and Dr. M. Mostoller, Dr. N. Lang and Dr. P. Lloyd for helpful discussions. Assistance in writing Clebsch-Gordan coefficient-computer programs by Dr. Harold Davis is gratefully acknowledged.

TABLE IV. Sensitivity of band parameters ($b\hat{p}$) to model potential parameters ($m\hat{p}\hat{p}$) [$\partial \ln(b\hat{p}) / \partial \ln(m\hat{p}\hat{p})$].

$\frac{\partial b\hat{p}}{\partial m\hat{p}\hat{p}}$	$\Delta_1^m - \Gamma_{25}'$	$L_1 - L_3'$	$\Gamma_{15} - \Gamma_{25}'$
α^a	-4.3	-0.4	-0.9
r_{0c}^b	-2.5	-4.0	0
r_{1c}^b	+8.9	+4.1	+1.0
$r_{2c} = r_{3c} = r_{4c}^b$	-0.2	-0.1	0

^a The one parameter adjusted to fit crystalline experimental data [defined in Eq. (38)].

^b The three parameters fit to ionic data [defined in Eq. (37)].

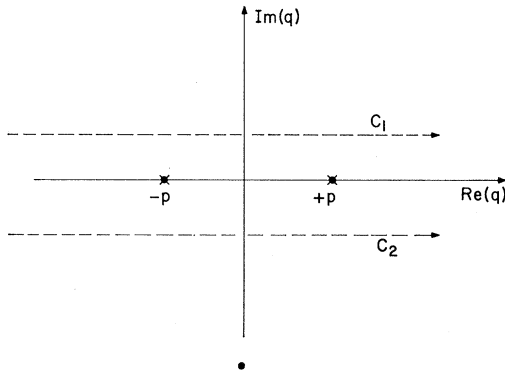


FIG. 3. The complex q plane discussed in conjunction with Eq. (A4).

APPENDIX A: EVALUATION OF $B_{L_1 L_2}(p, k, q)$

Substituting the completeness relation for plane waves into the definition of G' [Eq. (7)], we obtain

$$G'_{p\mathbf{k}}(\mathbf{r}_1 - \mathbf{r}_2) = (2\pi)^{-3} \sum_{\mathbf{R}} \sum' e^{i\mathbf{k} \cdot \mathbf{R}} \int d^3q (p^2 - q^2)^{-1} \times \exp[i\mathbf{q} \cdot (\mathbf{r}_1 - \mathbf{r}_2 - \mathbf{R})]. \quad (A1)$$

Letting $\mathbf{x} = \mathbf{r}_1 - \mathbf{r}_2$, we expand the plane wave in Eq. (A1) in real spherical harmonics

$$G_{p\mathbf{k}}'(\mathbf{x}) = 2\pi^{-1} \sum_{\mathbf{R}} e^{i\mathbf{k} \cdot \mathbf{R}} \sum_{L_1 L_2} i^{l_1 - l_2} Y_{L_1}(\hat{x}) Y_{L_2}(\hat{R}) \times \int d^3q (p^2 - q^2)^{-1} j_{l_1}(qx) j_{l_2}(qR) Y_{L_1}(\hat{q}) Y_{L_2}(\hat{q}). \quad (A2)$$

Performing the angular integration, we obtain

$$G_{p\mathbf{k}}'(\mathbf{x}) = \pi^{-1} \sum_{\mathbf{R}} e^{i\mathbf{k} \cdot \mathbf{R}} \sum_L Y_L(\hat{x}) Y_L(\hat{R}) \times \text{P.P.} \int_{-\infty}^{+\infty} q^2 dq (p^2 - q^2)^{-1} j_{l_1}(qx) j_{l_1}(qR), \quad (A3)$$

where the principal parts specification is dictated by our use of the standing-wave free-particle Green's function [Eq. (3)] and the extension of the lower limit of integration to $-\infty$ is permitted by the evenness of the integrand. We now replace the Bessel function $j_l(qR)$ by Hankel functions (the notation is that of Messiah,¹¹ p. 489) obtaining

$$\text{P.P.} \int_{-\infty}^{+\infty} q^2 dq (p^2 - q^2)^{-1} j_{l_1}(qx) j_{l_1}(qR) = (4i)^{-1} \int_{C_1 + C_2}^{+\infty} q^2 dq (p^2 - q^2)^{-1} j_{l_1}(qx) \times [h_l^+(qR) - h_l^-(qR)], \quad (A4)$$

where the contours C_1 and C_2 in the complex q plane are shown in Fig. 3. By replacing q by $-q$ we see that

$$\begin{aligned} \int_{C_1 + C_2} q^2 dq (p^2 - q^2)^{-1} j_{l_1}(qx) h_l^-(qR) \\ = - \int_{C_1 + C_2} q^2 dq (p^2 - q^2)^{-1} j_{l_1}(qx) h_l^+(qR) \end{aligned} \quad (A5)$$

and, therefore, that

$$\begin{aligned} \text{P.P.} \int_{-\infty}^{+\infty} q^2 dq (p^2 - q^2)^{-1} j_{l_1}(qx) j_{l_1}(qR) \\ = (2i)^{-1} \int_{C_1 + C_2} q^2 dq (p^2 - q^2)^{-1} j_{l_1}(qx) h_l^+(qR). \end{aligned} \quad (A6)$$

Deforming C_2 into C_1 and evaluating the residues at $q = \pm p$, we obtain

$$\begin{aligned} G_{p\mathbf{k}}'(\mathbf{x}) = \pi^{-1} \sum_{\mathbf{R}} e^{i\mathbf{k} \cdot \mathbf{R}} \sum_L Y_L(\hat{x}) Y_L(\hat{R}) \\ \times \left\{ -\pi p j_{l_1}(px) n_l(pR) - i \int_{C_1} q^2 dq (p^2 - q^2)^{-1} \right. \\ \left. \times j_{l_1}(qx) h_l^+(qR) \right\}. \end{aligned} \quad (A7)$$

We have now succeeded in separating G' into G^E and G^I , for we note that as long as $x < R$ the integrand in (A7) vanishes as $\text{Im}(q)$ goes to $+\infty$ causing the integral itself to vanish. The condition that $x = |\mathbf{r}_1 - \mathbf{r}_2| < R$ is, as mentioned in the text, just the mathematical specification of the muffin-tin restriction. To complete the identification of the first term in the brackets with G^E we use a relation easily derived from the plane-wave expansion formula:

$$\begin{aligned} i^l j_{l_1}(px) Y_L(\hat{x}) = 4\pi \sum_{L_1 L_2} C_{L_1 L_2 L} i^{l_1 - l_2} j_{l_1}(p\hat{r}_1) j_{l_2} \\ \times (p\hat{r}_2) Y_{L_1}(\hat{r}_1) Y_{L_2}(\hat{r}_2), \end{aligned} \quad (A8)$$

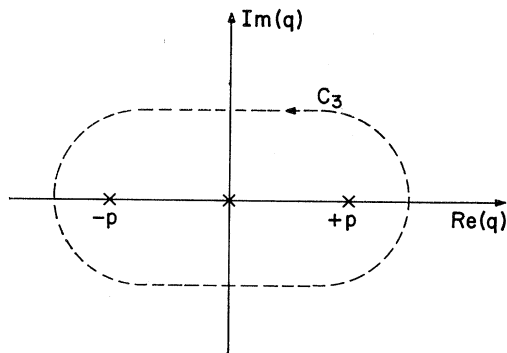


FIG. 4. The complex q plane discussed in conjunction with Eq. (A12).

where $C_{L_1 L_2 L} = \int d\hat{r} Y_{L_1}(\hat{r}) Y_{L_2}(\hat{r}) Y_L(\hat{r})$. Substituting (A8) into (A7) and recalling our definition of $B_{L_1 L_2 L}^E(p, \mathbf{k})$ [Eq. (15)], we obtain

$$B_{L_1 L_2 L}^E(p, \mathbf{k}) = i^{l_1 - l_2} (-4\pi p) \sum_L C_{L_1 L_2 L} i^{-l} \times \sum_{\mathbf{R}}' e^{i\mathbf{k} \cdot \mathbf{R}} n_l(pR) Y_L(\hat{R}) \quad (A9)$$

and

$$B_{L_1 L_2 L}^I(p, \mathbf{k}, \mathbf{r}_1, \mathbf{r}_2) = i^{l_1 - l_2} \sum_{\mathbf{R}}' e^{i\mathbf{k} \cdot \mathbf{R}} \sum_L C_{L_1 L_2 L} i^{-l} \times Y_L(\hat{R}) (-i) \int_{C_3} q^2 dq (p^2 - q^2)^{-1} j_{l_1}(qr_1) j_{l_2}(qr_2) \times (qr_2) h_l^+(qR). \quad (A10)$$

To evaluate the remaining integral and thereby obtain a useful formula for $B_{L_1 L_2 L}^I(p, \mathbf{k}, \mathbf{r}_1, \mathbf{r}_2)$, we decompose the remaining Bessel functions into Hankel functions:

$$j_{l_1}(qr_1) j_{l_2}(qr_2) = -4^{-1} [h_{l_1}^+(qr_1) h_{l_2}^+(qr_2) - h_{l_1}^+(qr_1) h_{l_2}^-(qr_2) - h_{l_1}^-(qr_1) h_{l_2}^-(qr_2) + h_{l_1}^-(qr_1) h_{l_2}^+(qr_2)]. \quad (A11)$$

If we restrict ourselves to spherically symmetric ionic potentials which are nonzero only for r less than the nearest-neighbor distance R_{NN} , then we need an expression for $B_{L_1 L_2 L}^I(p, \mathbf{k}, \mathbf{r}_1, \mathbf{r}_2)$ which is valid in the portion of the $\mathbf{r}_1, \mathbf{r}_2$ plane specified by $\mathbf{r}_1 + \mathbf{r}_2 > R_{NN}$ and $|\mathbf{r}_1 - \mathbf{r}_2| < R_{NN}$. In this portion of the $\mathbf{r}_1, \mathbf{r}_2$ plane we note that the first three terms in Eq. (A11) yield no contribution to the integral in Eq. (A10) and that for the fourth term we can close the contour in the lower half-plane. So, for the portion of the $\mathbf{r}_1, \mathbf{r}_2$ plane specified by $\mathbf{r}_1 + \mathbf{r}_2 > R_{NN}$ and $|\mathbf{r}_1 - \mathbf{r}_2| < R_{NN}$ we have

$$B_{L_1 L_2 L}^I(p, \mathbf{k}, \mathbf{r}_1, \mathbf{r}_2) = i^{l_1 - l_2} \sum_{L_3} C_{L_1 L_2 L} i^{-l} \sum_{\mathbf{R}}' e^{i\mathbf{k} \cdot \mathbf{R}} \times Y_L(\hat{R}) (-i) \int_{C_3} q^2 dq (p^2 - q^2)^{-1} \times h_{l_1}^-(qr_1) h_{l_2}^-(qr_2) h_l^+(qR), \quad (A12)$$

where the contour C_3 is shown in Fig. 4. (As suggested in Fig. 4 our decomposition of the Bessel functions has introduced a pole at the origin.) We can effect the final integration by distorting the contour C_3 so that $|q| > |p|$ everywhere on the contour and then expanding the various quantities in the integrand in power series about the origin. The relevant expansions are

$$h_{2\pm}(z) = \sum_{s=0}^l \frac{(\pm i)^{s-l} (l+s)!}{2^s s! (l-s)! z^s} \frac{e^{\pm i}}{z}, \quad (A13)$$

$$e^{-iq(r_1+r_2-R)} = \sum_{m=0}^{\infty} (m!)^{-1} [-iq(r_1+r_2-R)]^m, \quad (A14)$$

$$(p^2 - q^2)^{-1} = -q^2 \sum_{n=0}^{\infty} (p/q)^{2n}. \quad (A15)$$

Substituting these expressions into (A12) and using the following relation:

$$\int_{C_3} q^{n-1} dq = 2\pi i \delta(n), \quad (A16)$$

we arrive at the following expression:

$$B_{L_1 L_2 L}^I(p, \mathbf{k}, \mathbf{r}_1, \mathbf{r}_2) = i^{l_1 - l_2} \sum_L C_{L_1 L_2 L} (-)^l \times \sum_{\mathbf{R}}' e^{i\mathbf{k} \cdot \mathbf{R}} Y_L(\hat{R}) i^{l_1 + l_2} \pi \frac{(r_1 + r_2 - R)^2}{r_1 r_2 R} \times \left[\sum_{s_1=0}^{l_1} \frac{(l_1 + s_1)!}{(l_1 - s_1)! s_1!} \left(\frac{-(r_1 + r_2 - R)}{2r_1} \right)^{s_1} \sum_{s_2=0}^{l_2} \frac{(l_2 + s_2)!}{(l_2 - s_2)! s_2!} \right. \\ \left. \times \left(\frac{-(r_1 + r_2 - R)}{2r_2} \right)^{s_2} \sum_{s=0}^l \frac{(l+s)!}{(l-s)! s!} \left(\frac{r_1 + r_2 - R}{2R} \right)^s \right. \\ \left. \times \sum_{n=0}^{\infty} \frac{2[-E(r_1 + r_2 - R)^2]^n}{(2n + s_1 + s_2 + s + 2)!} \right]. \quad (A17)$$

We conclude this appendix by noting that G_{pk}' and more specifically the integral in Eq. (A3) arise not only in band theory but in any application of multiple-scattering theory (cf., Beeby,⁹ p. 86). This treatment of overlap can therefore be used virtually without alteration in the theory of disordered systems.

APPENDIX B: K-MATRIX AND SINGLE-CENTER SOLUTIONS

K_p is the transition matrix corresponding to the standing wave free-particle Green's function and therefore satisfies the analogous integral equations

$$K_p = v + K_p G_p^0 v. \quad (B1)$$

The corresponding integral equation for the single-center solution $|R_{lp}\rangle$ is

$$(1 - G_p^0 v) |R_{lp}\rangle = |Lp\rangle, \quad (B2)$$

where $|Lp\rangle$ is the free-particle solution of kinetic energy p^2 . The desired result [Eq. (33)] is obtained by operating on Eq. (B2) from the left with K_p :

$$v |R_{lp}\rangle = K_p |Lp\rangle. \quad (B3)$$

APPENDIX C: APPLICATION OF RPA SCREENING

Because of our lack of faith in the linear screening of strong potentials,³² we first isolate the long-range part of the ionic potential $v_{LR}(r)$ which is defined as follows:

$$v_{LR}(r) = -4r^{-1}\{1 - e^{-r/r_c}\},$$

where r_c is the average of the $\{r_{lc}\}$ introduced in

³² N. H. March and A. D. Boardman, *J. Phys. Soc. Japan Suppl.* II, 18, 80 (1963).

Eq. (37). $v_{LR}(r)$ was Fourier transformed to obtain $v_{LR}(q)$ which was then divided by the exchange-corrected RPA dielectric constant¹⁶ $\epsilon_{RPA}(q)$ to obtain the screened long-range potential $v_{SLR}(q)$. Using the fact that only values of $v_{SLR}(q)$ for q equal to nonzero reciprocal-lattice vectors are relevant to the band structure the irrelevant values of $v_{SLR}(q)$ were adjusted to further reduce the range of $v_{SLR}(r)$ which was finally obtained by Fourier transform. $v_{SLR}(r)$ was then recombined with the short-range part to produce the curve labeled RPA in Fig. 2.

Free-Carrier Optical Nonlinearity Due to Carrier Scattering and Nonparabolicity

M. S. SODHA, P. K. DUBEY, AND S. K. SHARMA

Physics Department, Indian Institute of Technology, Delhi, India

AND

P. K. KAW

Plasma Physics Laboratory, Princeton University, Princeton, New Jersey 08540

(Received 22 May 1969; revised manuscript received 20 October 1969)

Nonlinear mixing of electromagnetic waves in low-temperature degenerate semiconductors has been analytically investigated. Usual kinetic-theory techniques have been employed for evaluating the mixed-frequency components in the current density. Two types of free-carrier nonlinearity are considered, one arising from carrier scattering processes and the other due to nonparabolicity of conduction band. Numerical results, comparing the two nonlinearities for the special case of mixing of two CO₂ laser beams in indium antimonide, have been presented at the end.

1. INTRODUCTION

NONLINEAR harmonic generation and mixing of electromagnetic waves in semiconductors has been extensively studied both experimentally¹⁻⁵ and theoretically.⁶⁻¹⁴ It is well established now that at microwave and lower frequencies the free-carrier contribution to nonlinearity dominates the contribution arising from polarization of background lattice; the latter contribution seems to become important, in general, only at optical frequencies.¹⁵ Recent experi-

ments with indium antimonide and indium arsenide,⁵ however, indicate that for these materials free-carrier nonlinearity is the dominant nonlinearity, even at CO₂ laser frequencies (wavelengths 9.6 μ and 10.6 μ). Although this conclusion has been challenged,¹⁶ there can be no doubt that for many III-V compounds the free-carrier contribution to nonlinear phenomena is very important even at optical frequencies. In this paper we devote our attention exclusively to this type of nonlinearity in semiconductors.

Nonlinear phenomena of free carriers arise because of two different effects: (a) energy dependence of carrier relaxation time^{6-10,13,14} and (b) nonparabolicity of conduction band.^{11,12,17,18} For a semiconductor with a nonparabolic conduction band, both of these effects occur; however, the current theories⁶⁻¹³ of nonlinear harmonic generation and mixing seem to be restricted to either one or the other of these effects. It is the explicit purpose of the present paper to remove this restriction. Following Matz,¹⁷ the Boltzmann transfer equation for free carriers in a uniform isotropic semiconductor with spherical nonparabolic energy bands has been set up and solved by the usual Legendre-poly-

¹ K. Seeger, *J. Appl. Phys.* **34**, 1608 (1963).

² S. Kobayashi, S. Yabuki, and M. Aoki, *Japan J. Appl. Phys.* **2**, 127 (1963).

³ W. Schneider and K. Seeger, *Appl. Phys. Letters* **8**, 133 (1966).

⁴ G. Nimitz and K. Seeger, *J. Appl. Phys.* **39**, 2263 (1968).

⁵ C. K. N. Patel, R. E. Slusher, and P. A. Fleury, *Phys. Rev. Letters* **17**, 1011 (1966); J. J. Wynne, *Phys. Rev.* **178**, 1295 (1969).

⁶ B. V. Paranjape, *Phys. Rev.* **122**, 1372 (1961).

⁷ P. Das, *Phys. Rev.* **138**, A590 (1965).

⁸ M. S. Sodha and H. K. Srivastava, *Proc. Phys. Soc. (London)* **90**, 435 (1967).

⁹ M. S. Sodha, S. Sharma, and P. K. Kaw, *J. Phys. C* **1**, 1128 (1968).

¹⁰ P. K. Kaw, *J. Appl. Phys.* **40**, 793 (1969).

¹¹ P. A. Wolff and G. A. Pearson, *Phys. Rev. Letters* **17**, 1015 (1966).

¹² V. V. Paranjape and H. C. Law, *Phys. Letters* **25A**, 146 (1967).

¹³ P. K. Kaw, *Phys. Rev. Letters* **21**, 539 (1968).

¹⁴ M. S. Sodha and S. Sharma, *J. Phys. C* **2**, 914 (1969).

¹⁵ N. Bloembergen and Y. R. Shen, *Phys. Rev.* **141**, 298 (1966).

¹⁶ S. S. Jha and N. Bloembergen, *Phys. Rev.* **171**, 891 (1968).

¹⁷ D. Matz, *J. Phys. Chem. Solids* **28**, 373 (1967).

¹⁸ I. Lică, *Phys. Status Solidi* **25**, 461 (1968); **26**, 115 (1968).